Author/s:
Kolluri, RR;Mareels, I;de Hoog, J

Title:
Controlling DC microgrids in communities, buildings and data centers

Date:
2020-06-01

Citation:
Kolluri, R. R., Mareels, I. & de Hoog, J. (2020). Controlling DC microgrids in communities, buildings and data centers. IET Smart Grid, 3 (3), pp.376-384. https://doi.org/10.1049/iet-stg.2019.0281.

Persistent Link:
https://hdl.handle.net/11343/273956

IET Smart Grid

Research Article

IET Journals
The Institution of Engineering and Technology

Controlling DC microgrids in communities, buildings and data centers

eISSN 2515-2947
Received on 3rd October 2019
Revised 26th November 2019
Accepted on 16th March 2020
E-First on 15th May 2020
doi: 10.1049/iet-stg.2019.0281
www.ietdl.org

Ramachandra Rao Kolluri[1] ✉, *Iven Mareels*[1], *Julian de Hoog*[1]

[1]*IBM Research, IBM Australia Limited, Level 22, 60 City Road, Southbank, Victoria, Australia*

✉ *E-mail: rkolluri@au1.ibm.com*

Abstract: Microgrid technology is poised to transform the electricity industry. In the context of commercial/domestic buildings and data centers, where most loads are native direct current, DC microgrids are in fact a natural choice. Voltage stability and current/power-sharing between sources within a DC microgrid have been studied extensively in recent years. DC voltage droop control is known to have its drawbacks in that current or power-sharing is relatively poor. To eliminate this drawback, some have proposed to add a communication-based consensus control in addition to the primary voltage droop control loop. The current sharing performance is improved, however, the voltage deviation inherent in droop control requires a further, slower control to achieve voltage quality control. To overcome this complication, and reduction in response time, a low latency communication-based control technique that achieves proportional current sharing without significant voltage deviations is proposed in this work. The stability of the proposed control technique is compared to state-of-the-art using eigenvalue and transient analyses. The negative impact of communication delays on proposed control is discussed in detail.

1 Introduction

There has been a substantial increase in renewable energy based distributed generation and grid integration in recent years. Microgrids, which are defined as small, self-sustainable sections of the grid, become a natural extension of a distributed/decentralised generation paradigm. More importantly, given that a large proportion of the decentralised renewable energy comes from direct current (DC) sources, for example, rooftop solar photovoltaics systems, microgrids in DC form also become a straightforward application. The DC microgrid trend is also supported by a growing inclination towards low-cost energy-efficient devices such as LED lighting, switch-based systems such as servers, air-conditioners and so on, that primarily use DC form of energy. The majority of DC microgrid deployments are driven by reduced cost-of-conversion and increased overall efficiency. Currently, remote networks, often termed as *microgrids*, are attracting DC markets. Microgrids often include stand-alone buildings and data centers [1, 2]. Although there are some disadvantages associated with DC systems they remain out-of-scope for this work.

Research in the microgrid space has been expanding rapidly over the last few years. Given the advantages and simplicity of implementation, these trends are expected to increase over the next decade, paving new ways to integrate renewable energy into the power system and also revolutionising the traditional power system paradigm. One important research question is addressing how sources with local loads (prosumers) physically interact with each other in such situations. Control methods envisaged vary from communication independent central controller configuration to intelligent master–slave and intelligent master-less topologies. In this paper, the focus is on intelligently controlled master-less techniques used in operating DC microgrids.

1.1 Related work

The vast majority of early microgrid implementations were centred around AC systems. Droop control for paralleled AC systems was initially introduced in [3]. The primary motivation for this kind of control is the inherent speed-droop characteristic of a synchronous generator. Droop behaviour on the voltage and reactive power was also introduced in the same work. Inspired by this work there have been many papers focusing on operating multiple converter based sources in a network. The conceptual idea of microgrids, which was first introduced in [4], is also articulated around this droop control. Droop control, in an ideal scenario, is fully communication independent. The preliminary objective of control design in a microgrid (either AC or DC) is to maintain the system parameters (voltage and frequency for AC, voltage for DC) within acceptable limits. Lacking a strong source, like the *grid*, subsequent importance must be given to energy flexibility within the system. Power/energy sharing, therefore, becomes a fundamental objective in renewable or limited-energy microgrids. Power-sharing between sources in a DC microgrid has been the topic of research in many works [5–9]. Paralleling and interconnecting sources in a building microgrid for resiliency has been studied by some works [10]. Some works require explicit communication based supervisory control [7] while others use implicit forms of communication like power line signalling [6, 9]. Some works also use scheduling techniques to maintain power balance [11]. Ensuring proper power-sharing distribution between sources in a DC microgrid is subject to constituent line impedance distribution. The problem is analogous to reactive power-sharing in droop controlled AC microgrids [12, 13]. However, in DC systems it is a common strategy to design droop coefficients proportional to their line impedance distribution to achieve proper power-sharing. Increased focus on microgrid deployment together with the interest in improving network resilience, the advent of complex network configurations can be considered as certain. For complex networks where the impedance distribution is more scattered/unknown the estimation of line impedance is increasingly difficult. In [14] a decentralised method is presented to achieve improved current sharing based on the local rate of change of voltage. Distributed communication-based power/current sharing methods are also introduced in some works [5, 15–19]. However, voltage deviation from droop control cannot be avoided in most works since the current sharing control is implemented as a supplementary control loop to droop control or virtual impedance based control. However, with the advent of fast communication [20–22], primary control using nearest neighbour communications is achievable.

1.2 Contribution

In this work we revisit the stability and current sharing properties of existing control techniques in an attempt to develop a

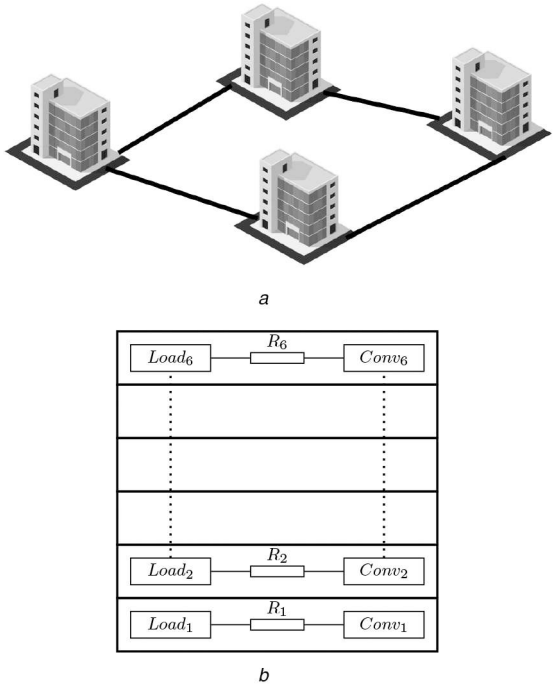

Fig. 1 *Microgrid applications*
(a) A high level representation of a community/campus/data center microgrid where different buildings are connected to each other for resiliency and power-sharing, ***(b)*** Building DC microgrid with floors operating on converter based sources and having interconnections for reliability. Converter based sources and loads are interconnected via line impedances to extend reliability

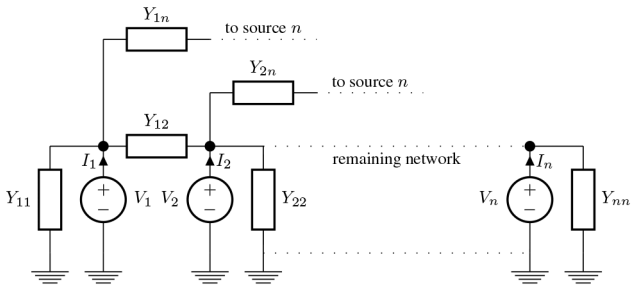

Fig. 2 *Reduced n source DC microgrid model. Each source has a local load of admittance Y_{ii} and is connected to all the remaining sources through lines of admittances Y_{ij}*

comprehensive comparative framework. Subsequently, we present the main contribution of this work - a new control technique that uses only nearest neighbour communication to achieve accurate current sharing at the expense of negligible voltage deviation. The communication only paradigm is inherently easy to implement in buildings, communities and data centers, which are envisaged as main avenues for application. Dynamic stability analysis is performed for all discussed controllers and conditions that guarantee stability in each case are listed. Eigenvalue analysis is performed to compare their performance and stability under communication delays in the proposed controller is also briefly addressed. A comparison is made between the proposed consensus current sharing method and an existing consensus power (CP)-sharing method using numerical analysis. This work is an elaborate version of our previous short paper [23] where a brief overview of the controller was provided. This work elaborates the setup, the controller and contains detailed proofs that establish stability conditions on the proposal while also comparing it with those of existing works, both theoretically and in simulations.

1.3 Organisation

The paper is organised as follows: Section 1 gives a brief introduction to the power-sharing problem being addressed backed up by a short review of some relevant literature. Section 2 gives a detailed technical description of the network model and the power-sharing problem under consideration. In Section 3 an elaboration on various control techniques is presented and corresponding state-space models are built. We also propose a technique which only uses neighbouring node information to control the voltage at each source. The stability properties are compared and dimensionality reduction is used to emphasise the existence of variable redundancy in consensus-based controllers. In Section 4 eigenvalue analysis is performed for an example network under each different control scenario. Impact of communication delay and power-sharing control that is analogous to current sharing control is briefly discussed. Simulation results are presented for all scenarios. Concluding remarks and future research directions are pointed out in Section 5. Here, some practical opportunities and implications are presented to broaden the technique's application spectrum.

2 Modelling

2.1 Preliminaries and notation

We define the n-dimensional column vector $\boldsymbol{x} = \text{col}(x_i) = [x_1, \ldots, x_n]^{\text{T}}$ where $(\cdot)^{\text{T}}$ represents a vector transpose function. $\mathbf{1}_n$ is an n-dimensional column vector of all ones. Let $\text{diag}(\text{col}(x_i))$ be a $(n \times n)$-dimensional diagonal matrix with x_i in the ith row and ith column and 0 elsewhere. The $(n \times n)$-dimensional identity matrix is given by $\boldsymbol{U} = \text{diag}(1_n)$. The matrix $\mathbf{1}_{n\times n}$ is a $(n \times n)$-dimensional matrix with all elements equal to 1. If $\underline{y} = a + \text{j}b$ is a complex number with $j = \sqrt{-1}$, then the real part is given by $\Re\{\underline{y}\} = a$ and the imaginary part is given by $\Im\{\underline{y}\} = b$. The notation $(\cdot)^*$ denotes complex conjugate of a complex number. A communication network is represented as a connected graph $\boldsymbol{G}_{\text{c}} = (\boldsymbol{V}_{\text{c}}, \boldsymbol{E}_{\text{c}})$, where $\boldsymbol{V}_{\text{c}}$ is the set of nodes and $\boldsymbol{E}_{\text{c}}$ is the set of edges which represent the communication links between nodes. We define the communication degree matrix $\boldsymbol{D}_{\text{c}} := \text{diag}(\deg(i))$, where $\deg(i)$ is the number of communication links connected to the ith node. Adjacency matrix $\boldsymbol{A}_{\text{c}}$ represents the connections between nodes in the communication graph with $a_{ij} = a_{ji} = 1$ if the nodes i and j are connected, and $a_{ij} = a_{ji} = 0$ otherwise. Self loops are avoided, meaning $a_{ii} = 0$ for any node i. The Laplacian associated with the communication graph is $\boldsymbol{L}_{\text{c}} = \boldsymbol{D}_{\text{c}} - \boldsymbol{A}_{\text{c}}$. The vector $\mathbf{1}_n$ is basis of the kernel of $\boldsymbol{L}_{\text{c}}$, i.e. for any vector $c = \theta 1_n, \theta \in \mathbb{R}\setminus\{0\}$ there is $\boldsymbol{L}_{\text{c}} c = 0_n$ and since the matrix is symmetric there is $c^{\text{T}}\boldsymbol{L}_{\text{c}} = 0_n^{\text{T}}$. Its eigenvalues $\{\lambda_{\text{c},1}, \lambda_{\text{c},2}, \ldots \lambda_{\text{c},n}\}$ obey the relationship [24]: $0 = \lambda_{\text{c},1} < \lambda_{\text{c},2} \leq \ldots \lambda_{\text{c},n}$.

2.2 Current sharing in DC microgrids

A DC source in this study is considered to be a bidirectional DC–DC converter attached to a battery. The battery is assumed to have an arbitrary capacity for the analysis since energy limitations are not considered, however, some limitations can be imposed in the form of power or current constraints as shown later in the paper. The model for the DC source is an average DC voltage which is based on the assumption that any high frequency switching dynamics average out over the time period of interest and the internal control loops (voltage only or cascaded voltage and current) are much faster than the control subsystems that change the reference voltage [25].

We define $\boldsymbol{S} = \{1, \ldots, n\}$ as the set of sources within the microgrid. Kron reduction is an abstract and convenient way of representing a network that contains constant impedance loads in an all-to-all source form with interconnection impedances and local loads (see Fig. 1 for an abstract example representation and Fig. 2 for a detailed interconnection example). This allows the formulation to be consistent with the physical network model used in this work. The internal impedance is also taken into account here. Using Kron reduction ([26]) any network that is considered in this work can be reduced to a topology where each voltage source, $V_i, \forall i \in \boldsymbol{S}$ is connected to a source $V_j, \forall j \in \boldsymbol{S}$ through an impedance R_{ij}. Resistances R_{ii} and/or R_{jj} represent resultant local loads.

The relationship between current flowing through voltage source V_i, I_i and the remaining network is given by

$$I_i = V_i Y_{ii} + \sum_{j=1}^{n} Y_{ij}(V_i - V_j). \tag{1}$$

Definition 1: Define

$$\boldsymbol{Y} := \begin{bmatrix} \sum_{j=1}^{n} Y_{1j} & \cdots & -Y_{1n} \\ \vdots & \ddots & \vdots \\ -Y_{n1} & \cdots & \sum_{j=1}^{n} Y_{nj} \end{bmatrix} \in \mathbb{R}^{n\times n}, \tag{2}$$

as a network admittance matrix. Also define current and voltage vectors as $\boldsymbol{I} := \mathrm{col}(I_i) \in \mathbb{R}^{n\times 1}$ and $\boldsymbol{V} := \mathrm{col}(V_i) \in \mathbb{R}^{n\times 1}$, respectively.

Based on Definition 1 and (2) it is possible to rewrite (1) in vector/matrix form as $\boldsymbol{I} = \boldsymbol{YV}$. It can be shown that the matrix $\boldsymbol{Y} \in \mathbb{R}^{n\times n}$ is positive definite using the Gershgorin circle theorem [18]. The power, P_i supplied by the ith source in such a symmetric Kron reduced network is given by

$$P_i = V_i^2 Y_{ii} + \sum_{j=1}^{n} V_i(V_i - V_j)Y_{ij}. \tag{3}$$

The power term, P_i is highly non-linear and consequently power-sharing correction is convoluted. The power vector can be defined as

$$\boldsymbol{P} := \mathrm{col}(P_i) = \mathrm{diag}(\boldsymbol{V})\boldsymbol{I} \in \mathbb{R}^{n\times 1}. \tag{4}$$

2.3 Droop (D) control

To enable decentralised voltage control [27] proposed DC droop or DC virtual impedance control. According to this control the voltage at each source, V_i is modified as follows:

$$V_i = V_{\mathrm{nom}} - m_i I_{\mathrm{f},i}, \tag{5}$$

where $V_{\mathrm{nom}>0}$ is a nominal DC voltage, $m_{i>0}$ is the DC virtual impedance/droop coefficient and $I_{\mathrm{f},i}$ is the filtered current output. Filtering the current term I_i to obtain $I_{\mathrm{f},i}$ serves two main purposes:

- helps avoid the voltage at each source being subject to rapid spikes or dips as an instant consequence of loading,
- adds virtual inertia to the microgrid network and thereby contributing to the overall stability (this shown later in this paper).

The filtered current variables are obtained as

$$\tau_i \dot{I}_{\mathrm{f},i} = -I_{\mathrm{f},i} + I_i, \tag{6}$$

where $\tau_{i>0}$ is the local low pass filter time constant.

Definition 2: We define the diagonal matrix of virtual impedances, diagonal matrix of filter time constants and filtered current vectors, respectively, as $\boldsymbol{M} := \mathrm{diag}(\mathrm{col}(m_i))$ $\boldsymbol{T} := \mathrm{diag}(\mathrm{col}(\tau_i) \in$ and $\boldsymbol{I}_{\mathrm{f}} := \mathrm{diag}(\mathrm{col}(I_{\mathrm{f},i})$.

Using Definition 2 it is possible to express vector forms of (5) and (6) as

$$\boldsymbol{V} = V_{\mathrm{nom}}\boldsymbol{1}_n - \boldsymbol{MI}_{\mathrm{f}},$$

$$\boldsymbol{T}\dot{\boldsymbol{I}}_{\mathrm{f}} = -\boldsymbol{I}_{\mathrm{f}} + \boldsymbol{I},$$

respectively. Writing the above equations together with the vector current equation yields

$$\boldsymbol{T}\dot{\boldsymbol{I}}_{\mathrm{f}} = -(\boldsymbol{U} + \boldsymbol{YM})\boldsymbol{I}_{\mathrm{f}} + V_{\mathrm{nom}}\boldsymbol{Y}\boldsymbol{1}_n.$$

The above system represents the simple droop-controlled DC microgrid, which is stable owing to the fact that the matrix $(\boldsymbol{U} + \boldsymbol{YM})$ is positive definite, thereby depicting the damping nature of the low-pass filter. Without the low pass filter for the current variables, the system would be modelled by purely algebraic equations.

2.4 Droop with consensus (D + C) controller

A consensus controller (structurally similar to that proposed in [19]) can be used to improve the current sharing attributes of simple droop controller. Each source implements the droop controller together with the consensus controller which is defined as

$$V_i = V_{\mathrm{nom}} - m_i I_{\mathrm{f},i} - z_i.$$

Here the consensus term, z_i is applied as negative feedback to the droop controller. The z_i are defined as the integral of the current imbalance as follows

$$\dot{z}_i = k_i \sum_{j\in N_i} (m_i I_{\mathrm{f},i} - m_j I_{\mathrm{f},j}) \tag{7}$$

where $k_i > 0$ is the integral control gain and $\boldsymbol{N}_i$ is the set of sources communicating with source i. Define the vector of integral control variables as

$$\boldsymbol{Z} := \mathrm{col}(z_1, \ldots, z_n) \in \mathbb{R}^{n\times 1}. \tag{8}$$

Assumption 1: Assume that the current measurement low-pass filter time constants of all sources are identical, i.e. $\boldsymbol{T}^{-1} = f\boldsymbol{U}$. We also assume that the integral control gains are identical, i.e. $k_i > 0 = k > 0, \forall i \in \boldsymbol{S}$.

Using (8) and Assumption 1 the vector dynamics of the integral controller (7) can be written as

$$\dot{\boldsymbol{Z}} = k\boldsymbol{L}_{\mathrm{c}}\boldsymbol{M}\boldsymbol{I}_{\mathrm{f}}.$$

Combining the dynamics of the filtered current and the integral control vectors yield

$$\begin{bmatrix} \dot{\boldsymbol{I}}_{\mathrm{f}} \\ \dot{\boldsymbol{Z}} \end{bmatrix} = \underbrace{\begin{bmatrix} -f(\boldsymbol{U} + \boldsymbol{YM}) & -f\boldsymbol{Y} \\ k\boldsymbol{L}_{\mathrm{c}}\boldsymbol{M} & \boldsymbol{0}_{n\times n} \end{bmatrix}}_{:=\boldsymbol{F}_{\mathrm{dc}}} \begin{bmatrix} \boldsymbol{I}_{\mathrm{f}} \\ \boldsymbol{Z} \end{bmatrix} + \begin{bmatrix} fV_{\mathrm{nom}}\boldsymbol{Y}\boldsymbol{1}_n \\ \boldsymbol{0}_n \end{bmatrix}. \tag{9}$$

2.5 Proposed consensus only (C) control

We propose a droop free consensus control which only relies on neighbouring node information. It uses the same integral controller and is given by

$$V_i = V_{\mathrm{nom}} - z_i.$$

In this manner, some robustness is lost in terms of decentralised control. However, given the proposal assumes close proximity of sources such as those in different levels of a building, community microgrids and data center microgrids, we may assume that the communication infrastructure is reliable and introduces little latency. Large voltage deviations as a result of system loading can be avoided in this manner. This will, in-turn, improve the steady-state current sharing performance of the microgrid and removes the need of subsequent secondary control in majority of the cases. The communications required for this type of control are generally faster than simple secondary control and common in microgrid

systems [20–22]. The dynamics of entire microgrid network with C control are given by

$$\begin{bmatrix}\dot{\boldsymbol{I}}_{\mathrm{f}}\\ \dot{\boldsymbol{Z}}\end{bmatrix}=\underbrace{\begin{bmatrix}-f\boldsymbol{U} & -f\boldsymbol{Y}\\ k\boldsymbol{L}_{\mathrm{c}}\boldsymbol{M} & \boldsymbol{0}_{n\times n}\end{bmatrix}}_{:=\boldsymbol{F}_{\mathrm{c}}}\begin{bmatrix}\boldsymbol{I}_{\mathrm{f}}\\ \boldsymbol{Z}\end{bmatrix}+\begin{bmatrix}fV_{\mathrm{nom}}\boldsymbol{Y}\boldsymbol{1}_n\\ \boldsymbol{0}_n\end{bmatrix}. \tag{10}$$

3 Dynamics and stability

In this section, the stability and steady-state behaviour of various control techniques are studied in extensive detail. The dynamics of a simple droop controlled microgrid (7) can be written as a single equation

$$\dot{\boldsymbol{I}}_{\mathrm{f}}=-\boldsymbol{T}^{-1}(\boldsymbol{U}+\boldsymbol{Y}\boldsymbol{M})\boldsymbol{I}_{\mathrm{f}}+\boldsymbol{C} \tag{11}$$

where $\boldsymbol{C}=V_{\mathrm{nom}}\boldsymbol{T}^{-1}\boldsymbol{Y}\boldsymbol{1}_n$. This system is stable for any practical choices of matrices $\boldsymbol{T}$ and $\boldsymbol{M}$ which result in positive definite $\boldsymbol{T}^{-1}\boldsymbol{Y}\boldsymbol{M}$. Following Assumption 1, the system dynamics can be rewritten as

$$\dot{\boldsymbol{I}}_{\mathrm{f}}=-f(\boldsymbol{U}+\boldsymbol{Y}\boldsymbol{M})\boldsymbol{I}_{\mathrm{f}}+\boldsymbol{C}_{\mathrm{f}}, \tag{12}$$

where $\boldsymbol{C}_{\mathrm{f}}=fV_{\mathrm{nom}}\boldsymbol{Y}\boldsymbol{1}_n$. The dynamics of the simple droop controlled system, as seen from (11) or (12), do not guarantee proportional current sharing mainly due to the offset introduced by $\boldsymbol{C}_{\mathrm{f}}$

$$\boldsymbol{I}_f^s=f^{-1}\boldsymbol{C}_{\mathrm{f}}(\boldsymbol{U}+\boldsymbol{Y}\boldsymbol{M})^{-1}.$$

3.1 Current sharing under consensus control

In stable steady-state, the integral controller, $\boldsymbol{Z}$ ensures proportional current sharing between sources in the microgrid in either D + C control or C control. To show this, recall that the communication Laplacian matrix $\boldsymbol{L}_{\mathrm{c}}$ is positive semi-definite with $(n-1)$ positive eigenvalues and a zero eigenvalue. The eigenvector ν associated with the zero eigenvalue is proportional to $\boldsymbol{1}_n$. So, in stable steady-state,

$$\dot{\boldsymbol{Z}}=k\boldsymbol{L}_{\mathrm{c}}\boldsymbol{M}\boldsymbol{I}_{\mathrm{f}}^s=\boldsymbol{0}_n,$$

$$\Rightarrow \boldsymbol{M}\boldsymbol{I}_{\mathrm{f}}^s=\alpha\boldsymbol{1}_n\Rightarrow m_iI_{\mathrm{f},i}^s=m_jI_{\mathrm{f},j}^s,$$

where α is the loading factor of the microgrid and $(\cdot)^s$ represents steady-state values. Subsequently, to prove the stability of the microgrid dynamics (9) or (10), the linear *state transition matrices* $\boldsymbol{F}_{\mathrm{dc}}$ or $\boldsymbol{F}_{\mathrm{c}}$ are analysed. It should be observed that a change the input vector $\boldsymbol{C}_{\mathrm{f}}$ will affect the equilibrium vector and consequently the system response. However, the stability arguments are presented against an arbitrary equilibrium vector and will therefore remain unaffected and consistent in $\boldsymbol{C}_{\mathrm{f}}$'s presence.

3.2 Stability of C control

Theorem 1: For a linearised state-space system approximated by *(10)*, its non-zero eigenvalues will always have a negative real part for any choice of $f>0$ and $k>0$.

Proof: To establish an understanding of system stability under C control, let us first consider the characteristic equation of $\boldsymbol{F}_{\mathrm{c}}$

$$\det\left(\lambda_{\boldsymbol{F}_{\mathrm{c}}}\boldsymbol{U}_{2n}-\boldsymbol{F}_{\mathrm{c}}\right)=\begin{vmatrix}(\lambda_{\boldsymbol{F}_{\mathrm{c}}}+f)\boldsymbol{U} & f\boldsymbol{Y}\\ -k\boldsymbol{L}_{\mathrm{c}}\boldsymbol{M} & \lambda_{\boldsymbol{F}_{\mathrm{c}}}\boldsymbol{U}\end{vmatrix},$$

where $\lambda_{\boldsymbol{F}_{\mathrm{c}}}$ is an eigenvalue of the matrix $\boldsymbol{F}_{\mathrm{c}}$. Using standard block matrix identities,

$$\det\left(\lambda_{\boldsymbol{F}_{\mathrm{c}}}\boldsymbol{U}_{2n}-\boldsymbol{F}_{\mathrm{c}}\right)=\det\left(\boldsymbol{Q}_{\mathrm{c}}(\boldsymbol{l}_{\boldsymbol{F}_{\mathrm{c}}})\right),$$

where $\boldsymbol{Q}_{\mathrm{c}}(\lambda_{\boldsymbol{F}_{\mathrm{c}}})$ is given by

$$\boldsymbol{Q}_{\mathrm{c}}(\lambda_{\boldsymbol{F}_{\mathrm{c}}})=\lambda_{\boldsymbol{F}_{\mathrm{c}}}^2\boldsymbol{U}+f\lambda_{\boldsymbol{F}_{\mathrm{c}}}\boldsymbol{U}+fk\boldsymbol{Y}\boldsymbol{L}_{\mathrm{c}}\boldsymbol{M}. \tag{13}$$

To compute the eigenvalues, let $v\in\mathbb{C}^n$ be any vector with $v^*v=1$. Left multiplying the characteristic polynomial (13) by v_i^* and right multiplying by $v_i, \forall i=1,\ldots,n$, yields

$$\lambda_{\boldsymbol{F}_{\mathrm{c}},i}^2+f\sigma_i\lambda_{\boldsymbol{F}_{\mathrm{c}},i}+fk\phi_i=0, \tag{14}$$

where $\sigma_i=1$ and $\phi_i=v_i^*(\boldsymbol{Y}\boldsymbol{L}_{\mathrm{c}}\boldsymbol{M})v_i$. We are particularly interested in two cases

(i) When $v_1=\boldsymbol{M}^{-1}\beta\boldsymbol{1}_n, \beta\in\mathbb{R}\setminus\{0\}$. Under this condition (14) becomes

$$\lambda_{\boldsymbol{F}_{\mathrm{c}},1}^2+f\sigma_i\lambda_{\boldsymbol{F}_{\mathrm{c}},1}=0.$$

This implies the eigenvalues $\lambda_{\boldsymbol{F}_{\mathrm{c}},1_1}=0$ and $\lambda_{\boldsymbol{F}_{\mathrm{c}},1_2}=-f$.

(ii) When $v_j\neq v_1, \forall j=2,3,\ldots,n$. The remaining $(2n-2)$ eigenvalues of $\boldsymbol{F}_{\mathrm{c}}$, $(\lambda_{\boldsymbol{F}_{\mathrm{c}},j}, \forall j=2,\ldots,n)$ are of the form

$$\lambda_{\boldsymbol{F}_{\mathrm{c}},j}=\frac{-f\pm\sqrt{(f^2-4kf\phi_j)}}{2}. \tag{15}$$

We can ensure (15) has eigenvalues of negative real part by imposing conditions on f, k and ϕ_j as follows:

Condition:

$$-f\pm\sqrt{(f^2-4kf\phi_j)}<0,$$
$$\pm\sqrt{(f^2-4kf\phi_j)}<f.$$

Squaring on both sides,

$$f^2-4kf\phi_j<f^2$$
$$\Rightarrow 4kf\phi_j>0.$$

The above condition can be achieved for simple choices of k and f greater than zero. □

3.3 Stability of D + C control

In a similar manner, let us now consider the characteristic equation of $\boldsymbol{F}_{\mathrm{dc}}$,

$$\det\left(\lambda_{\boldsymbol{F}_{\mathrm{dc}}}\boldsymbol{U}_{2n}-\boldsymbol{F}_{\mathrm{dc}}\right)=\begin{vmatrix}(\lambda_{\boldsymbol{F}_{\mathrm{dc}}}+f)\boldsymbol{U}+f\boldsymbol{Y}\boldsymbol{M} & f\boldsymbol{Y}\\ -k\boldsymbol{L}_{\mathrm{c}}\boldsymbol{M} & \lambda_{\boldsymbol{F}_{\mathrm{dc}}}\boldsymbol{U}\end{vmatrix},$$

where $\lambda_{\boldsymbol{F}_{\mathrm{dc}}}$ is an eigenvalue of the matrix $\boldsymbol{F}_{\mathrm{dc}}$. Using standard block matrix identities,

$$\det\left(\lambda_{\boldsymbol{F}_{\mathrm{dc}}}\boldsymbol{U}_{2n}-\boldsymbol{F}_{\mathrm{dc}}\right)=\det\left(\boldsymbol{Q}_{\mathrm{dc}}(\lambda_{\boldsymbol{F}_{\mathrm{dc}}})\right),$$

where

$$\boldsymbol{Q}_{\mathrm{dc}}(\lambda_{\boldsymbol{F}_{\mathrm{dc}}})=\lambda_{\boldsymbol{F}_{\mathrm{dc}}}^2\boldsymbol{U}+f\lambda_{\boldsymbol{F}_{\mathrm{dc}}}(\boldsymbol{U}+\boldsymbol{Y}\boldsymbol{M})+fk\boldsymbol{Y}\boldsymbol{L}_{\mathrm{c}}\boldsymbol{M}.$$

Let $v\in\mathbb{C}^n$ be any vector with $v^*v=1$. Left multiplying the characteristic polynomial (13) by v_i^* and right multiplying by $v_i, \forall i=1,\ldots,n$, yields

$$\lambda_{\boldsymbol{F}_{\mathrm{dc}},i}^2+f\mu_i\lambda_{\boldsymbol{F}_{\mathrm{dc}},i}+fk\phi_i=0,$$

where $\mu_i = v_i^*(\boldsymbol{U} + \boldsymbol{YM})v_i$ and $\phi_i = v_i^*(\boldsymbol{YL}_c\boldsymbol{M})v_i$ (A slight abuse of notation - repeated usage of ϕ to preserve consistency in qualitative arguments). Observe that (16) and(13) have a similar structure except the first order term is different. The smallest value of μ_i is generally larger than unity which may contribute to improving the overall stability. To evaluate, the eigenvalues are

$$\lambda_{\boldsymbol{F}_{\mathrm{dc}},1_1} = 0, \lambda_{\boldsymbol{F}_{\mathrm{dc}},1_2} = -f\mu_1, \text{and}$$

$$\lambda_{\boldsymbol{F}_{\mathrm{dc}},j} = \frac{-f\mu_j \pm \sqrt{(f^2\mu_j^2 - 4kf\phi_j)}}{2}, \quad \forall j = 2, \ldots, n\,.$$

The condition for stability remains the same as the droop free consensus control scenario. The steady-state voltage of the droop + consensus controller is lower than that of the C controller by a factor of $\boldsymbol{MI}_{\mathrm{f}}^s$ which is dependent on system loading. This will in-turn lower the overall power consumption in the microgrid owing to the constant impedance load type chosen for analysis.

Remark 1: Strictly speaking, Assumption 1 is not essential. The stability result will remain unchanged, as may be gleaned from a continuity argument (as long as T^{-1} is positive definite, and k_i is strictly positive). In this view, k and f are extracted to explicitly emphasise their impact to eigenvalue evolution.

Remark 2: From a stability point of view, consensus controller design, as formulated in this work, will only benefit from a detailed knowledge of $\boldsymbol{Y}$. It is understood that detailed impedance information is hard to obtain in some cases, especially as the networks grow in size. However, lacking such information does not present a limitation to the controller design.

Remark 3: The proposed consensus controller acts on current sharing mismatches between itself and its neighbours, and, in that sense, we can add linear energy (integral on local current) constraints into the controller. This can be envisioned as a way to elaborate the arbitrary battery capacity assumption. However, separate controllers have to be designed to guarantee stability on the constraint boundary, i.e. to drive the state evolution into the stable region once they intersect a constraint boundary and reach an integral saturation. In an alternative method, we can tune the convergence time and offshoot of the presented controller to minimise energy deviation. Exhaustive evaluation of these approaches is interesting future work.

3.4 Zero eigenvalue in the presence of consensus controller - heuristic argument

The zero eigenvalue of the state transition matrix ($\boldsymbol{F}_{\mathrm{c}}$ or $\boldsymbol{F}_{\mathrm{dc}}$) signifies a redundancy of variables that arise from the introduction of distributed communication-based control. We can eliminate the zero eigenvalue using dimensionality reduction. To do this, from (7),

$$\dot{z}_1 = -k_1 \sum_{i=2}^{n} \frac{\dot{z}_i}{k_i}$$

Assuming the integral control variables are starting at zero initial condition,

$$z_1 = -k_1 \sum_{i=2}^{n} \frac{z_i}{k_i}$$

Based on Assumption 1 made earlier, the above equation can be rewritten as

$$z_1 = -\sum_{i=2}^{n} z_i$$

This reduces the dimension of state transition matrix ($\boldsymbol{F}_{\mathrm{c}}$ or $\boldsymbol{F}_{\mathrm{dc}}$) to $\mathbb{R}^{(2n-1)\times(2n-1)}$ from $\mathbb{R}^{2n\times 2n}$. Define

$$\boldsymbol{U}_{(n-1)} := \mathrm{diag}(1, \ldots, 1) \in \mathbb{R}^{(n-1)\times(n-1)},$$

$$\boldsymbol{R}_0 := \mathrm{row}(\boldsymbol{0}_{(n-1)}, \boldsymbol{U}_{(n-1)}) \in \mathbb{R}^{(n-1)\times n},$$

$$\hat{\boldsymbol{Z}} := \mathrm{col}(z_2, \ldots, z_n) \in \mathbb{R}^{(n-1)},$$

$$\tilde{\boldsymbol{1}}_{(n-1)} := \mathrm{col}(1, \ldots, 1)^{\mathrm{T}} \in \mathbb{R}^{1\times(n-1)},$$

$$\boldsymbol{X} := \mathrm{col}(\tilde{\boldsymbol{1}}_{(n-1)}, -\boldsymbol{U}_{n-1}) \in \mathbb{R}^{n\times(n-1)}.$$

Matrices $\boldsymbol{F}_c$ or $\boldsymbol{F}_{\mathrm{dc}}$ can now be represented in a form where the redundant variables are eliminated.

$$\frac{\mathrm{d}}{\mathrm{d}t}\begin{bmatrix}\boldsymbol{I}_f\\ \hat{\boldsymbol{Z}}\end{bmatrix} = \underbrace{\begin{bmatrix}* & -f\boldsymbol{YX}\\ k\boldsymbol{R}_0\boldsymbol{L}_c\boldsymbol{M} & \boldsymbol{0}_{(n-1)\times(n-1)}\end{bmatrix}}_{:=\boldsymbol{F}}\begin{bmatrix}\boldsymbol{I}_{\mathrm{f}}\\ \hat{\boldsymbol{Z}}\end{bmatrix} + \begin{bmatrix}\boldsymbol{C}_{\mathrm{f}}\\ \boldsymbol{0}_{(n-1)}\end{bmatrix}.$$

By using Cauchy Binet formula the determinant of $\boldsymbol{F} \in \mathbb{R}^{(2n-1)\times(2n-1)}$ is given by $|kf\boldsymbol{R}_0\boldsymbol{L}_c\boldsymbol{MYX}|$ [28]. Since $\boldsymbol{L}_c$ is the only matrix with a zero eigenvalue and the basis of the kernel of $\boldsymbol{L}_c$ cannot be mapped through $\boldsymbol{R}_0$ or $\boldsymbol{X}$, it is apparent that the determinant is not zero, signifying the absence of a zero eigenvalue. The redundancy introduced cannot be avoided unless one source does not participate in implementing the consensus controller. However, in doing so, the microgrid cannot claim fully distributed operation any further. The redundancy in states therefore indirectly implies fully distributed mode of operation, in this case. Fully distributed operation is important and desirable as it provides the benefit of being able to retro-fit and expand a microgrid without having to reconfigure the control laws. The basis of the argument presented here is not limited to any equilibrium point, but may require work to prove stability for a given equilibrium point.

3.5 Impact of communication delay

Communications introduce small delays in the system model. Analysis that includes communication delay becomes increasingly hard for large networks [16]. Applying communication only techniques for controlling DC microgrids is more reliable when compared to their AC counterparts owing to the time-sensitiveness of the latter's parameters, especially frequency and phase [29, 30]. Using the formulation as shown below, the impact of delay on the system can be characterised using numerical methods. A complete analysis for time delays that depend on the network topology, and may themselves vary over time due to communication network loading is prohibitive. Here we restrict ourselves to point to some robustness with respect to delays in the communication network. In general we may conclude that in view of the stability with no time delay there exists a time delay t_d^* such that for all time delays $t_{d_i} < t_d^*$ the system will perform well. To further support this statement, we consider a system with a single time delay across all communication links:

Let us consider the delay t_d is time invariant and homogeneous throughout the communication network. Since only neighbouring node communication is utilised, the integral consensus controller can be rewritten as

$$\dot{z}_i(t) = k_i \sum_{j\in N_i} \left(m_i I_{i,\mathrm{f}}(t) - m_j I_{j,\mathrm{f}}(t - t_{\mathrm{d}})\right), \tag{16}$$

in the presence of communication delay. This emphasises that the local variables are available instantaneously but the variables that are obtained through a communication channel are delayed. This model accurately represents a homogeneous communication delay, however, the computation delay etc., are assumed insignificant and neglected.

Definition 3: In this section, we define the time-dependent state vector $\boldsymbol{x}(t) := \boldsymbol{x}_t$. Similarly, we also define a delayed state-vector as $\boldsymbol{x}(t - t_\mathrm{d}) = \boldsymbol{x}_{\mathrm{t,d}}$.

Using Definition 3, the matrix form of (16) can be represented as

$$\boldsymbol{Z}_t = k\boldsymbol{D}_c\boldsymbol{M}\boldsymbol{I}_{ft} - k\boldsymbol{A}_c\boldsymbol{M}\boldsymbol{I}_{ft,d} \tag{17}$$

Plugging the delay differential equation (DDE) (17) in the system dynamics (10) yields a new set of DDEs

$$\begin{bmatrix}\dot{\boldsymbol{I}}_{ft}\\ \dot{\boldsymbol{Z}}_t\end{bmatrix} = \begin{bmatrix}-f\boldsymbol{U} & -f\boldsymbol{Y}\\ k\boldsymbol{D}_\mathrm{c}\boldsymbol{M} & \boldsymbol{0}_{n\times n}\end{bmatrix}\begin{bmatrix}\boldsymbol{I}_\mathrm{ft}\\ \boldsymbol{Z}_t\end{bmatrix} + \begin{bmatrix}\boldsymbol{0}_{n\times n} & \boldsymbol{0}_{n\times n}\\ -k\boldsymbol{A}_\mathrm{c}\boldsymbol{M} & \boldsymbol{0}_{n\times n}\end{bmatrix}\begin{bmatrix}\boldsymbol{I}_{\mathrm{ft,d}}\\ \boldsymbol{Z}_{\mathrm{t,d}}\end{bmatrix} + \begin{bmatrix}\boldsymbol{C}_\mathrm{f}\\ \boldsymbol{0}_n\end{bmatrix}.$$

These equations are of the form

$$\dot{\boldsymbol{x}}_\mathrm{t} = \boldsymbol{A}\boldsymbol{x}_t + \boldsymbol{A}_\mathrm{d}\boldsymbol{x}_{\mathrm{t,d}} + \boldsymbol{u}, \tag{18}$$

where $\boldsymbol{u}$ represents inputs to the system. According to [31] eigenvalues, λ of (18) are the solutions of:

$$\det\left(\lambda\boldsymbol{U} - \boldsymbol{A} - \boldsymbol{A}_\mathrm{d}\mathrm{e}^{-\lambda t_\mathrm{d}}\right) = \boldsymbol{0}.$$

There are infinitely many solutions to the above equation owing to the exponential term which makes analytically constructing the stability based on eigenvalues impractical. Numerical solution for the equations can be obtained by using various DDE solvers [31].

4 Simulation experiments

Multiple simulations are conducted to validate the performance of the proposal. We only compare the results of the proposal with D + C control technique given that D + C technique is quite superior (in current sharing terms) to techniques like D control or control-less systems. The microgrid network used in the simulation experiments is given in Fig. 3. The network is connected all-to-all with each source having a local load to supply, a scenario representative of building or data-center microgrids. This, consequently, also represents a Kron reduced network thereby making it directly compatible with the analysis presented earlier. Recall that the objective of the controllers is to achieve current sharing. The design of the droop coefficient matrix $\boldsymbol{M}$ is based on maximum voltage deviation allowed and maximum current that can be supplied by each source. The sources have an identical rating, $I_\mathrm{max} = \pm 40\,\mathrm{A}$ (representative of a 16 kW bidirectional source at each node), nominal voltage, $V_\mathrm{nom} = 400\,\mathrm{V}$ and the maximum local deviation allowed, $\Delta V = \pm 10\,\mathrm{V}$. This makes $\boldsymbol{M} = 0.25\boldsymbol{U}$ V/A, a choice that also represents equal current sharing. The filter cut-off frequency is $f = 10\,\mathrm{Hz}$ and the initial value for the integral control gain $k = 1$.

The network is loaded heavily and these parameters along with the line parameters are represented by the admittance matrix:

$$\boldsymbol{Y} \simeq \begin{bmatrix}31.74 & -10 & -5 & -10 & -6.67\\ -10 & 45.1 & -10 & -5 & -20\\ -5 & -10 & 28.4 & -10 & -3.34\\ -10 & -5 & -10 & 35.04 & -10\\ -6.67 & -20 & -3.34 & -10 & 40.2\end{bmatrix}\Omega^{-1}.$$

From Fig. 3, observe that the Laplacian matrix $\boldsymbol{L}_\mathrm{c}$ is of the form

$$\boldsymbol{L}_\mathrm{c} = \begin{bmatrix}1 & -1 & 0 & 0 & 0\\ -1 & 2 & -1 & 0 & 0\\ 0 & -1 & 2 & -1 & 0\\ 0 & 0 & -1 & 2 & -1\\ 0 & 0 & 0 & -1 & 1\end{bmatrix}.$$

of $\boldsymbol{Y}$ are [0.09, 33.33, 38.69, 43.60, 64.75] and of $\boldsymbol{L}_\mathrm{c}$ are [0, 0.3820, 1.3820, 2.6180, 3.6180]. The system eigenvalues for given parameters are shown in Table 1. As seen from the table, the eigenvalues of the C controller are all in the range of $-f/2$ with some imaginary part. As deduced in the analysis, there always is a real eigenvalue - f and a zero eigenvalue representing redundancy. Increasing the control gain k in the C controller changes the oscillatory response of the system as the imaginary part is only affected. Although most of the eigenvalues of the D + C controller have smaller real parts (larger negative values), the limiting eigenvalues have real parts that are larger than the largest real parts of eigenvalues in the C control system. Increasing the control gain k from 1 to 10 causes some oscillatory nodes in the D + C control system, however the limiting eigenvalues are still larger than the C control type. A very large increase in the control gain k will make the response more oscillator in either case. However the speed of convergence remains almost identical due to the fact that there are a few eigenmodes that are independent of the control gain k. The matrix $\boldsymbol{M}$ has a dominant effect on these modes in the D + C control.

4.1 Stability and power-sharing capability

The network as shown in Fig. 3 is simulated on MATLAB Simulink to analyse the transient stability of various control techniques. Communication links, indicated by the dotted blue lines in Fig. 3, are chosen to be discrete data streams at 1 kHz frequency (1 sample every millisecond) without any measurement

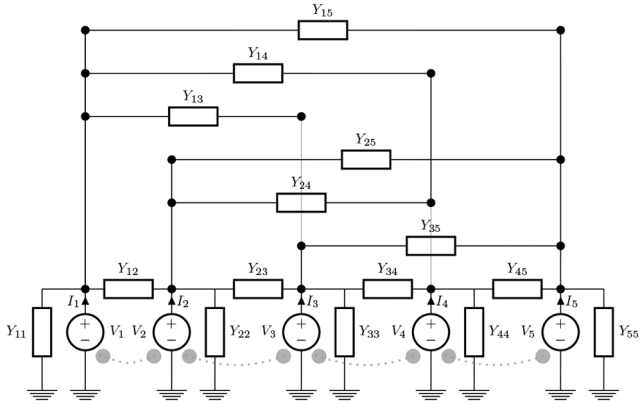

Fig. 3 *Reduced 5 source DC microgrid model. Communication links between sources are shown using grey dotted lines*

Table 1 Eigenvalues of the network model with different controllers (C = consensus only, $D + C$ = droop + consensus) and different integral control gains; (left) $k = 1$; and (right) $k = 10$

$\boldsymbol{C}$, $\lambda_{\boldsymbol{F}_\mathrm{c}}$	$\boldsymbol{D}+\boldsymbol{C}$, $\lambda_{\boldsymbol{F}_\mathrm{dc}}$	$\boldsymbol{C}$, $\lambda_{\boldsymbol{F}_\mathrm{c}}$	$\boldsymbol{D}+\boldsymbol{C}$, $\lambda_{\boldsymbol{F}_\mathrm{dc}}$
−5 + 21.57j	−169.67	−5 + 69.84j	−149.6
−5 − 21.57j	−117.48	−5 − 69.84j	−100
−5 + 15.37j	−104.71	−5 + 50.9j	−73
−5 − 15.37j	−91.62	−5 − 50.9j	−57.45 + 14.74j
−5 + 10.09j	−10.22	−5 + 35.28j	−57.45 − 14.74j
−5 − 10.09j	−3.45	−5 − 35.28j	−35.11
−5 + 4.32j	−2.43	−5 + 20.29j	−14.52
−5 − 4.32j	−1.26	−5 − 20.29j	−10.22
−10	−0.35	−10	−3.61
0	0	0	0

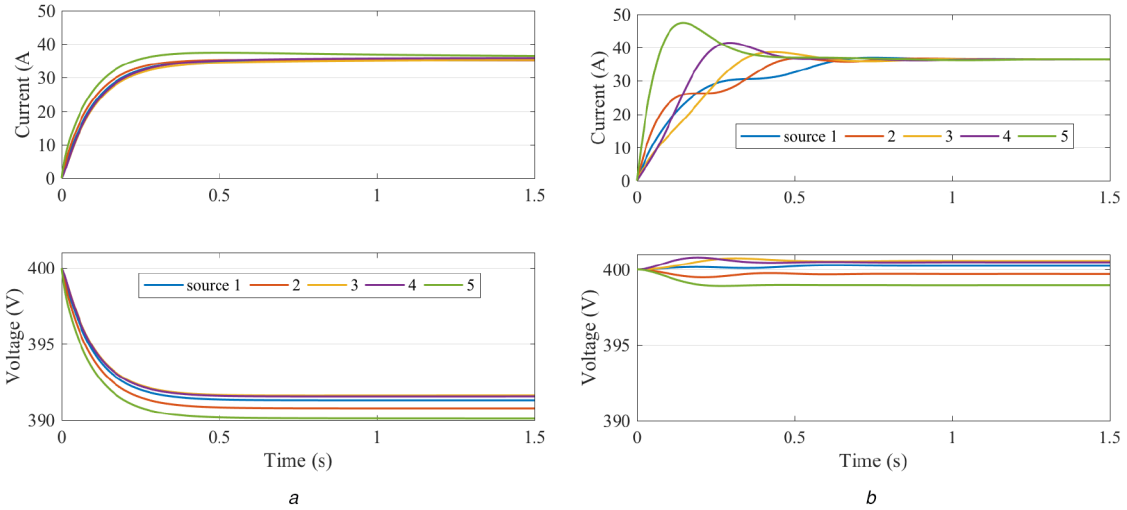

Fig. 4 *Comparison between output currents and voltages of the simulation example under two different control techniques with integral control gain $k = 1$*
(a) Droop + consensus control, ***(b)*** Consensus control only

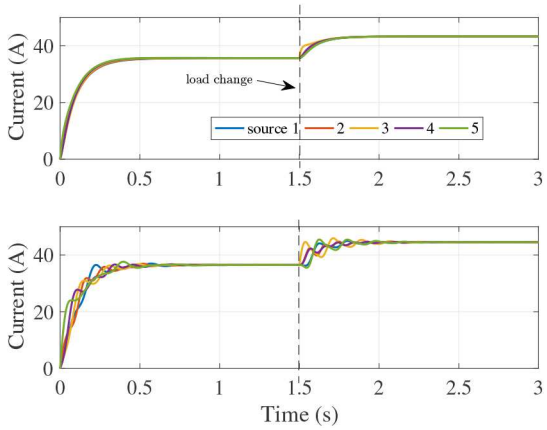

Fig. 5 *Current sharing performance for increased control gain $k = 10$ (top) D + C control; and (bottom) C control. Load increase occurs at time t = 1.5 s*

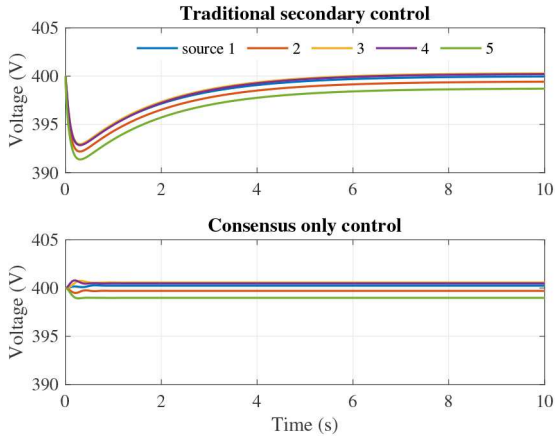

Fig. 6 *Comparing voltage regulation in standard secondary control to the proposed consensus controller*

noise. In Fig. 4, droop + consensus control technique is compared with the proposed C control.

When $k = 1$, it can be seen that the droop control based technique in Fig. 4*a* has higher voltage deviation and slower speed of convergence than that of the C technique (as shown in Fig. 4*b*). When $k = 10$ the convergence speed of D + C control is comparable with C control with either value of k. Increasing the control gain k introduces an oscillatory response as suggested by its eigenvalues in Table 1, but the convergence speed remains identical to the case where $k = 1$. This is indicated by the real part of the eigenvalues as they remain unmodified. The oscillatory modes in the D + C control at $k = 10$ subside relatively faster owing to the larger real part of the complex conjugate eigenvalues. The steady-state voltage deviation with $k = 10$ at time $t = 1.5$ s is exactly the same as in the case with $k = 1$ under C control. This is because the integral term impact is disabled naturally under equilibrium, i.e. z_i^* approaches zero in steady-state. Both techniques are not destabilised by reasonable perturbations (load changes) as shown in Fig. 5 ($1.5\text{ s} < t \leq 3\text{ s}$). We cannot guarantee stability with respect to larger perturbations as the linearity is typically violated and analysis disintegrates under any such extreme conditions.

C control does not require secondary control to correct voltage deviation as latter is negligible. It is to be noted that the oscillatory response of C control is the only variable that can be controlled by a reasonable increase in k owing to its position in (16). A steep increase in k might lead to enormous oscillations, which might eventually render the microgrid unstable owing to the over-current protection system interventions. The power-sharing performance of both the control techniques is comparable, however in absolute terms the C control has higher power values owing to the smaller voltage deviations and the constant impedance load type. In cases where the voltage is deliberately reduced to achieve lower power consumption (for example, conservation voltage reduction [32]) the C control can be used with lower nominal voltage values rather than making the voltage explicitly dependent on loading.

In most standard secondary control techniques an anchor node tries to regulate its voltage to a known nominal value, preferably V_{nom}, thereby effectively leading to overall microgrid voltage regulation. Standard secondary control acts at a much slower time-scale to avoid interference with primary current/power sharing controllers. A simulation result where the source V_3 is chosen as the anchor node to perform standard secondary control is given in Fig. 6. It can be seen that the voltage regulation performance of standard secondary controller is comparable to the proposed consensus only control, albeit being 7 s slower, highlighting the latter's efficiency.

4.2 Performance for various communication delays

In this paper simulation results are presented to show the impact of communication delays on the stability of the given network in Fig. 3 with C control. The delay is introduced using a standard delay block in SIMULINK library. Fig. 7 (top) shows the response of the constituent sources with $t_{\text{d}} = 20$ ms delay on the communication channel (comparable to practical system delays [33]). Filtered currents converge to a common constant value within 2 s. However, when the delay $t_{\text{d}} = 200$ ms, the filtered current states shoot exponentially, as shown in Fig. 7 (bottom), rendering the network unstable.

The simulation results are unrealistic in a sense that in practice the sources will be protected against over-currents, and switch off before damage can be done. Nevertheless, instability is not acceptable, as it makes the network non-functional.

4.3 Power-sharing using consensus only control

Considering power-sharing instead of current sharing conforms better with practical limitations. As seen earlier, power-sharing is non-linear due to the presence of a product term in (4). Identical to the C control, consensus only control can be used for power-sharing purposes as well. We term this type of control as CP control. Let us consider power-sharing, where the power is measured using a low pass filter and the associated dynamics are given by

$$\tau_{\mathrm{p}}\dot{P}_{i,\mathrm{f}} = -P_{i,\mathrm{f}} + P_i,$$

where τ_{p} is the low pass filter time constant, $P_{i,\mathrm{f}}$ is the filtered power and P_i is given by (3). The consensus controller (i.e. based on delay independent neighbouring node N_{i} communication) can be defined as

$$\dot{z}_{i,\mathrm{p}} = k_{i,\mathrm{p}} \sum_{j \in N_i} (m_{i,\mathrm{p}} P_{i,f} - m_{j,\mathrm{p}} P_{j,\mathrm{f}})$$

where $z_{i,\mathrm{p}}$ integral power controller, $k_{i,\mathrm{p}}$ is the control gain and $m_{i,\mathrm{p}}$ is the power-sharing coefficient. The new integral control variable $z_{i,\mathrm{p}}$ is added as negative feedback to the voltage as

$$V_{\mathrm{i}} = V_{\mathrm{nom}} - z_{i,\mathrm{p}}.$$

Defining vectors and matrices as shown earlier will result in the matrix form of the consensus only power-sharing system:

$$\dot{\boldsymbol{P}}_{\mathrm{f}} = -f_{\mathrm{p}}\boldsymbol{P}_{\mathrm{f}} + f_{\mathrm{p}}\mathrm{diag}(\boldsymbol{V})\boldsymbol{Y}\boldsymbol{V},$$

$$\dot{\boldsymbol{Z}}_{\mathrm{p}} = k_{\mathrm{p}}\boldsymbol{L}_{\mathrm{c}}\boldsymbol{M}_{\mathrm{p}}\boldsymbol{P}_{\mathrm{f}},$$

$$\boldsymbol{V} = V_{\mathrm{nom}}\boldsymbol{1}_n - \boldsymbol{Z}_p.$$

We can prove small-signal stability of the CP controller by considering a linearisation argument similar to that made in [34]. The term diag($\boldsymbol{V}$) is close to the nominal voltage $V_{\mathrm{nom}}\boldsymbol{U}$ since there is no droop control implemented. This linearised system dynamics of CP control are as follows:

$$\begin{bmatrix}\dot{\boldsymbol{P}}_{\mathrm{f}}\\ \dot{\boldsymbol{Z}}_{\mathrm{p}}\end{bmatrix} = \underbrace{\begin{bmatrix}-f\boldsymbol{U} & -fV_{\mathrm{nom}}\boldsymbol{Y}\\ k_{\mathrm{p}}\boldsymbol{L}_{\mathrm{c}}\boldsymbol{M} & \boldsymbol{0}_{n\times n}\end{bmatrix}}_{:=\boldsymbol{F}_{\mathrm{cp}}}\begin{bmatrix}\boldsymbol{P}_f\\ \boldsymbol{Z}_{\mathrm{p}}\end{bmatrix} + \begin{bmatrix}\boldsymbol{C}_{\mathrm{p}}\\ \boldsymbol{0}_n\end{bmatrix},$$

where $\boldsymbol{C}_{\mathrm{p}} = fV_{\mathrm{nom}}^2\boldsymbol{Y}\boldsymbol{1}_n$. The stability of the CP control technique translates to the stability of C control if we replace k_p by k/V_{nom}.

Power-sharing for the network shown in Fig. 3 with the three different techniques is compared in Fig. 8. Since CP control achieves accurate power-sharing, it has been chosen as the benchmark. For the present example, D + C control is within approximately −4.5% power deviation from the benchmark, while C control (current only) is within ±0.4%. Therefore, it can be concluded that CP control and C control are comparative in power-sharing performance and low voltage deviation. However, proving global stability of the CP control requires further analysis (for example, see [15]) due to the non-linearity in power dynamics.

To summarise, as seen from Table 2, considerable voltage drops occur in droop based control which can be avoided by consensus only controls. Although current sharing capabilities are comparable qualitatively, quantitative differences are prominent due to constant impedance load type along with discrepancies in voltage.

5 Conclusion

Designing and controlling DC microgrids within buildings and campuses is a step closer towards making them efficient, self-sustainable, resilient and carbon neutral. Power-sharing and inter-dependent operation between sources in such microgrids helps us leverage their flexibility. It is well known that steady-state current-sharing between voltage sources in a DC microgrid with constant

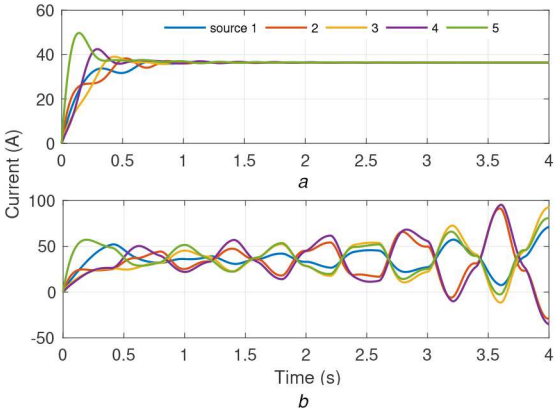

Fig. 7 *Current sharing performance of C control in the presence of communication delay*
(a) Communication delay $t_{\mathrm{d}} = 20$ ms, ***(b)*** Communication delay $t_{\mathrm{d}} = 200$ ms

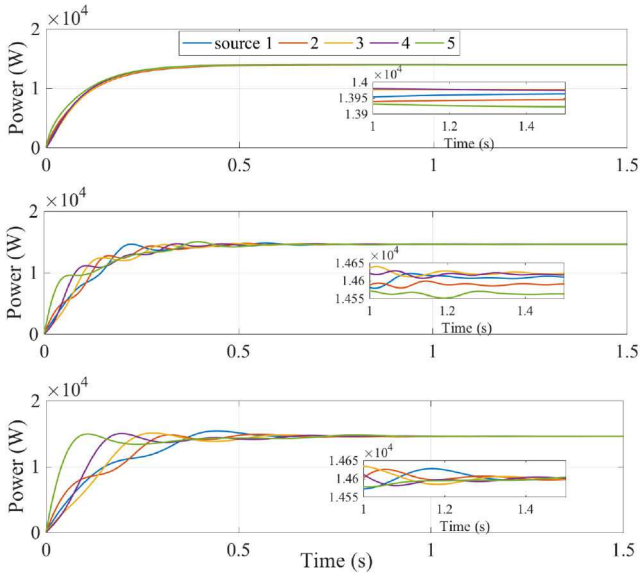

Fig. 8 *Power-sharing performance of (top) D + C control with $m_i = 0.25$ V/A and $k = 10$; (middle) C control with $m_i = 0.25$ V/A and $k = 10$; and (bottom) CP control with $m_{i,p} = 0.25$ V/W and $k_{\mathrm{p}} = 10/V_{\mathrm{nom}}$*

Table 2 Quasi-steady-state value ranges for various control types after time $t = 5$ s.

Parameter	NC	D	D + C	C	CP
V_{max}, V	400	383.06	391.6	400.6	400.6
V_{min}, V	400	381.6	390.1	399	399
I_{max}, A	80	36.76	35.68	36.49	36.59
I_{min}, A	16	34.02	35.68	36.49	36.44

NC = no control

impedance loads depends on the network parameters. This is not desirable in a microgrid scenario, and in order to use the available infrastructure properly, it is essential that both voltage stability and (appropriate) current-sharing is achieved simultaneously. To this end additional control is required to manage the current distribution.

In this paper, the performance of droop + consensus control in DC microgrid is compared with a newly proposed technique that uses consensus only control. It is shown that the current-sharing performance of both controllers are similar, observing that the consensus only controller is significantly simpler. Power-sharing, and voltage control, however, perform better using the simpler C controller precisely because it provides for smaller voltage deviations. Stability conditions for this control are presented. Redundancy in the integral control variables gives rise to a zero eigenvalue overall. It is justified using a dimensionality reduction argument. Redundancy is an essential feature allowing the microgrid to be expanded without having to redesign the control laws. A simulation example supports the theoretical developments. In conclusion, C control can be used to advantage in microgrids when the speed of current convergence has a lower priority than voltage stability. The control requires that the communication infrastructure is reliable and does not introduce significant latency. Since in C control systems the voltage is controlled to be closer to its nominal value, the overall power consumption is close to what the load requires, and may be greater than in droop + consensus control.

Finally, a brief and incomplete analysis was carried out for power-sharing control using consensus only control. A comprehensive analysis of the impact of communication latency on the overall dynamics as well as a complete non-linear stability analysis of power-sharing consensus control are the subject of further study.

6 References

[1] Asmus, P.: 'Data centers and advanced microgrids: meeting resiliency, efficiency, and sustainability goals through smart and cleaner power infrastructure', *Navigant Res.*, 2017, **1**, pp. 1–31

[2] Thompson, C.C., Konstantinos Oikonomou, P.E., Etemadi, A.H., *et al.*: 'Optimization of data center battery storage investments for microgrid cost savings, emissions reduction, and reliability enhancement', *IEEE Trans. Ind. Appl.*, 2016, **52**, (3), pp. 2053–2060

[3] Chandorkar, M., Divan, D., Adapa, R.: 'Control of parallel connected inverters in standalone ac supply systems', *IEEE Trans. Ind. Appl.*, 1993, **29**, (1), pp. 136–143

[4] Peas Lopes, J., Moreira, C., Madureira, A.: 'Defining control strategies for microgrids islanded operation', *IEEE Trans. Power Syst.*, 2006, **21**, (2), pp. 916–924

[5] Anand, S., Fernandes, B.G., Guerrero, M.: 'Distributed control to ensure proportional load sharing and improve voltage regulation in low-voltage dc microgrids', *IEEE Trans. Power Electron.*, 2013, **28**, (4), pp. 1900–1913

[6] Dragicevic, T., Guerrero, J., Vasquez, J.: 'A distributed control strategy for coordination of an autonomous lvdc microgrid based on power-line signaling', *IEEE Trans. Ind. Electron.*, 2014a, **61**, (7), pp. 3313–3326

[7] Dragicevic, T., Guerrero, J., Vasquez, J., *et al.*: 'Supervisory control of an adaptive-droop regulated dc microgrid with battery management capability', *IEEE Trans. Power Electron.*, 2014b, **29**, (2), pp. 695–706

[8] Liu, Y., Wang, J., Li, N., *et al.*: 'Enhanced load power sharing accuracy in droop-controlled dc microgrids with both mesh and radial configurations', *Energies*, 2015, **8**, (5), p. 3591

[9] Pinomaa, A., Ahola, J., Kosonen, A.: 'Power-line communication-based network architecture for lvdc distribution system'. IEEE Int. Symp. on Power Line Communications and Its Applications (ISPLC), Udine, Italy, 2011, pp. 358–363

[10] Ma, T., Yahoui, H., Vu, H., *et al.*: 'A control strategy of dc building microgrid connected to the neighborhood and ac power network', *Buildings*, 2017, **7**, (2), p. 42

[11] Wang, P., Jin, C., Zhu, D., *et al.*: 'Distributed control for autonomous operation of a three-port ac/dc/ds hybrid microgrid', *IEEE Trans. Ind. Electron.*, 2015, **62**, (2), pp. 1279–1290

[12] Schiffer, J., Seel, T., Raisch, J., *et al.*: 'Voltage stability and reactive power sharing in inverter-based microgrids with consensus-based distributed voltage control', *IEEE Trans. Control Syst. Technol.*, 2016, **24**, (1), pp. 96–109

[13] Zambroni de Souza, A.C., Santos, M., Castilla, M., *et al.*: 'Voltage security in ac microgrids: a power flow-based approach considering droop-controlled inverters', *IET Renew. Power Gener.*, 2015, **9**, (8), pp. 954–960

[14] Yang, J., Jin, X., Wu, X., *et al.*: 'Decentralised control method for dc microgrids with improved current sharing accuracy', *IET Gener. Transm. Distrib.*, 2017, **11**, (3), pp. 696–706

[15] Han, R., Aldana, N.L.D., Meng, L., *et al.*: 'Droop-free distributed control with event-triggered communication in dc micro-grid'. 2017 IEEE Applied Power Electronics Conf. and Exposition (APEC), Tampa, FL, USA, 2017, pp. 1160–1166

[16] Lu, X., Guerrero, J.M., Sun, K., *et al.*: 'An improved droop control method for dc microgrids based on low bandwidth communication with dc bus voltage restoration and enhanced current sharing accuracy', *IEEE Trans. Power Electron.*, 2014, **29**, (4), pp. 1800–1812

[17] Morstyn, T., Hredzak, B., Demetriades, G.D., *et al.*: 'Unified distributed control for dc microgrid operating modes', *IEEE Trans. Power Syst.*, 2016, **31**, (1), pp. 802–812

[18] Xiang, J., Li, Y., Wei, W.: 'Stability analysis of dc microgrids with cooperative droop control'. 2016 35th Chinese Control Conf. (CCC), Chengdu, China, 2016, pp. 9963–9968

[19] Zhao, J., Dörfler, F.: 'Distributed control and optimization in dc microgrids', *Automatica*, 2015, **61**, pp. 18–26

[20] Gungor, V.C., Sahin, D., Kocak, T., *et al.*: 'Smart grid technologies: communication technologies and standards', *IEEE Trans. Ind. Inf.*, 2011, **7**, (4), pp. 529–539

[21] Laaksonen, H.J.: 'Protection principles for future microgrids', *IEEE Trans. Power Electron.*, 2010, **25**, (12), pp. 2910–2918

[22] Xin, H., Qu, Z., Seuss, J., *et al.*: 'A self-organizing strategy for power flow control of photovoltaic generators in a distribution network', *IEEE Trans. Power Syst.*, 2011, **26**, (3), pp. 1462–1473

[23] Kolluri, R.R., Mareels, I., de Hoog, J.: 'Consensus only control in dc microgrids'. Proc. Ninth Int. Conf. on Future Energy Systems, e-Energy '18, New York, NY, USA, 2018, pp. 423–425

[24] Olfati-Saber, R., Fax, J., Murray, R.: 'Consensus and cooperation in networked multi-agent systems', *Proc. IEEE*, 2007, **95**, (1), pp. 215–233

[25] Holmes, D., Lipo, T.: '*Pulse width modulation for power converters: principles and practice*'. IEEE Press Series on Power Engineering (John Wiley & Sons, USA, 2003)

[26] Dorfler, F., Bullo, F.: 'Kron reduction of graphs with applications to electrical networks', 2011

[27] Guerrero, J.M., Vasquez, J.C., Matas, J., *et al.*: 'Hierarchical control of droop-controlled ac and dc microgrids: A general approach toward standardization', *IEEE Trans. Ind. Electron.*, 2011, **58**, (1), pp. 158–172

[28] Broida, J., Williamson, S.: '*A comprehensive Introduction to linear algebra*'. Advanced Book Program. (Addison-Wesley, USA, 1989)

[29] Kolluri, R.R., Mareels, I., Alpcan, T., *et al.*: 'Power sharing in angle droop controlled microgrids', *IEEE Trans. Power Syst.*, 2017, **32**, (6), pp. 4743–4751

[30] Schiffer, J., Ortega, R., Hans, C.A., *et al.*: 'Droop-controlled inverter-based microgrids are robust to clock drifts'. 2015 American Control Conf. (ACC), Chicago, IL, USA, 2015, pp. 2341–2346

[31] Coelho, E.A.A., Wu, D., Guerrero, J.M., *et al.*: 'Small-signal analysis of the microgrid secondary control considering a communication time delay', *IEEE Trans. Ind. Electron.*, 2016, **63**, (10), pp. 6257–6269

[32] Pasha, A.M., Zeineldin, H.H., Al-Sumaiti, A.S., *et al.*: 'Conservation voltage reduction for autonomous microgrids based on *v-i* droop characteristics', *IEEE Trans. Sustain. Energy*, 2017, **8**, (3), pp. 1076–1085

[33] Sayani, M.A.G., Singh, B.K., Coulter, J., *et al.*: 'Segment wise communication delay measurement for smart grid applications'. 2014 27th Biennial Symp. on Communications (QBSC), Kingston, ON, USA, 2014, pp. 139–143

[34] Simpson-Porco, J.W., Shafiee, Q., Dörfler, F., *et al.*: 'Secondary frequency and voltage control of islanded microgrids via distributed averaging', *IEEE Trans. Ind. Electron.*, 2015, **62**, (11), pp. 7025–7038